xuv resonant transition radiations from periodic stratified media

J.-M. André,[1] B. Pardo,[2] and C. Bonnelle[1]
[1]*Laboratoire de Chimie Physique-Matière et Rayonnement, Université Pierre et Marie Curie, UMR-CNRS 7614, 11 rue Pierre et Marie Curie, 75231 Paris Cedex 05, France*
[2]*Institut d'Optique Théorique et Appliquée, Université Paris–Sud, CNRS, Laboratoire Associé 14, Campus d'Orsay, 91403 Orsay Cedex, France*
(Received 7 April 1998; revised manuscript received 12 February 1999)

General formulation of the xuv intensity emitted when relativistic electrons cross through any periodic stratified medium is presented in the framework of electromagnetism in continuous media. Application is made to the resonant transition radiation emitted in the geometries of both normal and oblique incidence. In the first case, agreement is found between our calculated results and published values. Intensity emitted by a periodic multilayer stack used in the Bragg conditions is determined and the practical interest of a such a radiation source is discussed. [S1063-651X(99)08007-1]

PACS number(s): 41.60.−m

I. INTRODUCTION

When a fast charged particle travels through an optically heterogeneous medium, an electromagnetic radiation is emitted [1–3]. This emission is a consequence of the readjustment of the field associated with the charged particle when it moves in a material showing a sudden change, or a gradient, of polarization. Such a change exists at the interface between two media and, consequently, x-ray emission, named transition radiation (TR), has been observed when relativistic electrons cross a stack of thin foils [4–7]. The emission takes place in a narrow cone centered on the electron direction and having angular spread of the order $1/\gamma=(1-\beta^2)^{1/2}$. For incident electrons of 10 to 100 MeV, the emission lies in the soft-x-ray energy range.

Conditions giving intense transition radiation have been researched [8–10]. Periodic arrangements of interfaces have been proposed. Indeed, when the distance between the interfaces is such that the waves emitted at different interfaces interfere constructively, an enhancement of radiation occurs and this is named resonant transition radiation (RTR) [11–13]. Coherence of the transition radiation leading to an intensity enhancement has been observed. In these experiments, incident electrons cross perpendicularly stacks of thin foils and only interfaces between low atomic number material and vacuum have been experimented. The period of such systems cannot be lower than some microns and the fabrication of this kind of radiator is no easy task. Moreover, irregularities in the spacing between the foils can rapidly destroy the coherence of the emission.

An alternative method has been proposed [14–16]. In this method, the radiator is a periodic multilayered structure. Preliminary theoretical study of the radiation emitted by a stratified structure, crossed by an incident particle perpendicularly to the layer planes, has been made. It suggests that particular phenomena should occur in the vicinity of the Bragg conditions [15,17]. On the other hand, it is well known that xuv radiation of a chosen wavelength can be reflected in the Bragg conditions by multilayered arrangements. The principal aim of this paper is to show theoretically that xuv transition radiation can be obtained from periodic multilayer and geometry in which both relativistic charged particles and radiation have directions satisfying the Bragg conditions. We refer to this emission as *Bragg resonant* transition radiation (Bragg RTR).

In the hard x-ray range, crystals are used as Bragg diffractors and it has been theoretically shown that hard x-ray radiation is emitted when a relativistic charged particle impinges through a monocrystal in conditions close to the Bragg direction [18–24]. This phenomenon was designed as parametric x-ray radiation (PXR). Dialetis [18] has developed a theoretical model valuable to describe the PXR but no numerical values of intensity have been calculated from his model. Independently models have been proposed and used for comparison with the PXR experimental results [25–33].

In this paper, starting from a model which treat the process in the framework of the classical electromagnetism [18], we establish the general expression of the radiative energy emitted by a stratified medium during the crossing by a relativistic electron in any incidence angle. Moreover, we show that our model accounts for both RTR and Bragg RTR. Our model assumes that the incident beam is not perturbed by the presence of the material and the energy lost by the particle is negligible compared with its kinetic energy. These approximations are usual for fast particles. Because the system under consideration is a stratified medium described in the framework of continuous media, our final expression is not directly applicable to crystals.

From the analytical expression that we obtain, a first calculation is performed in the spectral range of 1 keV for a periodic stack of Be films separated by the vacuum and crossed perpendicularly by an electron. The calculated intensity is compared with the previous published values [34]. Agreement is good at the precision of the optical constants in this energy range. A second calculation is made in the same spectral range for an artificial periodic multilayer structure crossed by an electron in the Bragg conditions. The number of photons radiated by an actual periodic structure [35] is compared with the intensity of the synchrotron radiation at the same energy.

The paper is organized as follows. Section II is devoted to establishing general formulas giving the electromagnetic intensity radiated by a charged particle moving uniformly through a multilayer stack. In Sec. III we establish the main

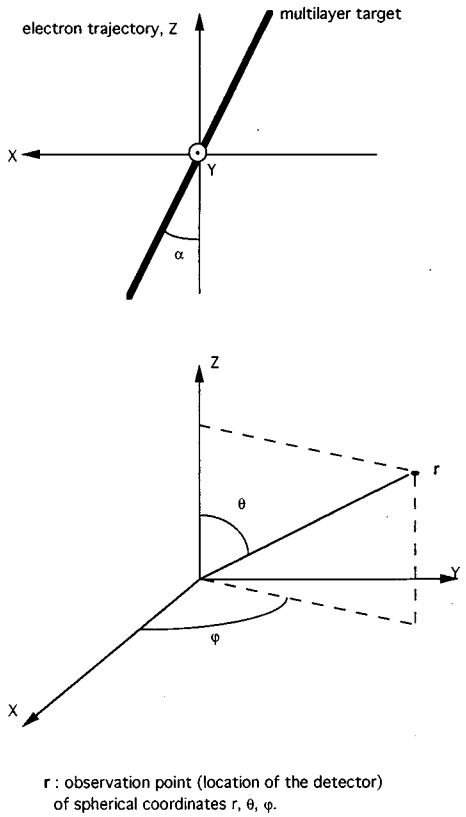

FIG. 1. Geometry of the problem.

formulas useful for a qualitative discussion of both RTR and Bragg RTR. Numerical examples and comparison with synchrotron radiation are given in Sec. IV and conclusion in Sec. V.

II. RADIATED ENERGY

We treat the problem in the framework of the electromagnetism of continuous media within the Gaussian unit system; c is the celerity of light in vacuum. The optical properties of the medium at a point $\mathbf{R}$ for the angular frequency ω are described by the dielectric constant, or electric permittivity, $\varepsilon(\mathbf{R},\omega)$. In the spectral range of interest, the magnetic permeability μ of the medium is equal to unity. We consider an electrically charged particle—in practice an electron—of charge denoted q, moving through a periodic medium with the constant velocity $\mathbf{v}$. β stands for v/c. The geometry and the relevant notations of the problem are given in Fig. 1. The medium is made up of alterned layers of material a and material b. The period of the structure, that is, the sum of the thickness of the layer a and of the thickness of the layer b, is denoted by d. The particle travels through the (X,Z) plane along the Z direction, which makes the angle α with the plane of the layers. The observation point $\mathbf{r}$ has the spherical coordinates r,θ,φ.

The electric $\mathbf{E}(\mathbf{r},\omega)$ and magnetic $\mathbf{H}(\mathbf{r},\omega)$ fields can be obtained from the electric Hertz vector $\mathbf{\Pi}(\mathbf{r},\omega)$ according to (cf. Appendix A)

$$\mathbf{E}(\mathbf{r},\omega)=\boldsymbol{\nabla}\times\boldsymbol{\nabla}\times\Pi(\mathbf{r},\omega)-4\pi\mathbf{P}(\mathbf{r},\omega)-i\frac{4\pi}{\omega}\mathbf{J}(\mathbf{r},\omega)$$

$$\times\mathbf{H}(\mathbf{r},\omega)=-ik\boldsymbol{\nabla}\times\mathbf{\Pi}(\mathbf{r},\omega), \tag{1}$$

where $k=\omega/c$ is the wave number in vacuum. $\mathbf{J}(\mathbf{R},\omega)$ is the time-Fourier transform of the current associated with the traveling particle and $\mathbf{P}(\mathbf{R},\omega)$ is the polarization vector induced by the traveling charged particle. At the location of the observator, that is, outside of the matter and of the electron beam, $\mathbf{P}(\mathbf{r},\omega)$ and $\mathbf{J}(\mathbf{r},\omega)$ vanish.

Let us recall that the vector $\mathbf{P}(\mathbf{R},\omega)$ is related to the electric field $\mathbf{E}(\mathbf{R},\omega)$ through the dielectric susceptibility $\chi(\mathbf{R},\omega)$ by the relation

$$\mathbf{P}(\mathbf{R},\omega)=\chi(\mathbf{R},\omega)\mathbf{E}(\mathbf{R},\omega) \tag{2}$$

and the susceptibility is related to the dielectric constant $\varepsilon(\mathbf{R},\omega)$ by

$$\chi(\mathbf{R},\omega)=\frac{\varepsilon(\mathbf{R},\omega)-1}{4\pi}. \tag{3}$$

The electric Hertz vector obeys the following differential equation (cf. Appendix A):

$$\boldsymbol{\nabla}^2\mathbf{\Pi}(\mathbf{r},\omega)+k^2\mathbf{\Pi}(\mathbf{r},\omega)=-4\pi\mathbf{P}(\mathbf{r},\omega)-i\frac{4\pi}{\omega}\mathbf{J}(\mathbf{r},\omega) \tag{4}$$

whose solution is given in terms of the outgoing Green function $G(\mathbf{r},\mathbf{R},\omega)$ of the Helmholtz equation by

$$\mathbf{\Pi}(\mathbf{r},\omega)=\int\left(\mathbf{P}(\mathbf{R},\omega)+\frac{i}{\omega}\mathbf{J}(\mathbf{R},\omega)\right)G(\mathbf{r},\mathbf{R},\omega)d^3\mathbf{R}. \tag{5}$$

The interest of the Hertz vector formulation is to lead straightforwardly to a method that we call the ''mean-field'' approximation. In this approach, the following applies.

(i) At large distance of the material, i.e., in the far-field approximation, only the component of the Hertz vector associated with the polarization vector $\mathbf{P}$ is important so that the relevant Hertz vector can be written

$$\mathbf{\Pi}(\mathbf{r},\omega)=\frac{\exp(ikr)}{r}\overline{\mathbf{\Pi}}(\mathbf{k},\omega) \tag{6}$$

with

$$\overline{\mathbf{\Pi}}(\mathbf{k},\omega)=\int\chi(\mathbf{R},\omega)\mathbf{E}(\mathbf{R},\omega)\exp(-i\mathbf{k}\cdot\mathbf{R})d^3\mathbf{R}, \tag{7}$$

where

$$\mathbf{k}=k\hat{\mathbf{r}}=\mathbf{k}(\sin\theta\cos\varphi\hat{\mathbf{X}}+\sin\theta\sin\varphi\hat{\mathbf{Y}}+\cos\theta\hat{\mathbf{Z}}). \tag{8}$$

$\hat{\mathbf{r}}$ and $\mathbf{k}$ are, respectively, the unit vector and the wave vector in the observation direction.

(ii) The electric field $\mathbf{E}(\mathbf{R},\omega)$ in the integrand of Eq. (7) is approximated by the electric field $\mathbf{E}_0(\mathbf{R},\omega)$ radiated by the electron moving uniformly in a ''mean'' medium of spatially averaged dielectric constant $\overline{\varepsilon(\omega)}=1+4\pi\overline{\chi}$. In these conditions, $\overline{\mathbf{\Pi}}(\mathbf{k},\omega)$ is given by

$$\overline{\mathbf{\Pi}}(\mathbf{k},\omega)\approx\int\chi(\mathbf{R},\omega)\mathbf{E}_0(\mathbf{R},\omega)\exp(-i\mathbf{k}\cdot\mathbf{R})d^3\mathbf{R}. \tag{9}$$

The energy radiated in far-field per unit frequency interval $d\omega$ and per steradian $d\Omega$ is expressed in terms of $\overline{\mathbf{\Pi}}(\mathbf{k},\omega)$ as follows (cf. Appendix B):

$$\frac{d^2I}{d\omega\, d\Omega}=\frac{c}{(2\pi)^2}k^4\left|\{\overline{\mathbf{\Pi}^*}(\mathbf{k},\omega)\cdot\overline{\mathbf{\Pi}}(\mathbf{k},\omega)-[\overline{\mathbf{\Pi}^*}(\mathbf{k},\omega)\cdot\hat{\mathbf{r}}]\times[\overline{\mathbf{\Pi}}(\mathbf{k},\omega)\cdot\hat{\mathbf{r}}]\}\right|, \tag{10}$$

where $*$ stands for the complex conjugation.

The expression of the electric field $\mathbf{E}_0$, radiated by an electron traveling uniformly through the medium of dielectric constant $\overline{\varepsilon(\omega)}$, is given in electromagnetic textbooks [36,37]. One notes that $\mathbf{E}_0$ has a radial symmetry along the Z axis and its radial $E_0^\rho(\rho,\omega)$ and longitudinal $E_0^Z(\rho,\omega)$ components are, respectively,

$$E_0^\rho(\rho,\omega)=\frac{2q}{v}\frac{\Lambda}{\overline{\overline{\varepsilon(\omega)}}}K_1(\Lambda\rho)\exp\left(i\frac{\omega}{v}Z\right),$$
$$E_0^Z(\rho,\omega)=-i\frac{2q}{\omega}\frac{\Lambda^2}{\overline{\overline{\varepsilon(\omega)}}}K_0(\Lambda\rho)\exp\left(i\frac{\omega}{v}Z\right), \tag{11}$$

where $\rho=\sqrt{X^2+Y^2}$ is the distance to the electron trajectory, K_1 and K_0 are the first- and zero-order Bessel function, and

$$\Lambda=\frac{k}{\beta}\sqrt{[1-\beta^2\overline{\varepsilon(\omega)}]}=k\left(\frac{1}{(\gamma\beta)^2}+4\pi\overline{\chi}\right)^{1/2}, \tag{12a}$$

where γ is the Lorentz parameter:

$$\gamma=\frac{1}{\sqrt{1-\beta^2}}. \tag{12b}$$

In the limit case where $\overline{\varepsilon(\omega)}$ tends toward unity (case of vacuum), Λ becomes

$$\Lambda=\frac{k}{\beta\gamma}. \tag{13}$$

For a periodic material of period d, the susceptibility can be expanded in Fourier series:

$$\chi(\mathbf{R},\omega)=\sum_{p=-\infty}^{+\infty}\chi_p(\omega)\exp(ipg_X X)\exp(ipg_Z Z), \tag{14}$$

where

$$g_X=\frac{2\pi}{d}\cos\alpha,$$
$$g_Z=\frac{2\pi}{d}\sin\alpha, \tag{15}$$

and

$$\chi_0(\omega)=\frac{\overline{\varepsilon(\omega)}-1}{4\pi},$$
$$\chi_p(\omega)=\exp(-ip\pi\Gamma)\frac{\Delta\chi(\omega)}{p\pi}\sin(\Gamma p\pi),\quad p\neq 0. \tag{16}$$

$\chi_p(\omega)$ is obtained as the Fourier transform of the susceptibility profile and $\Delta\chi(\omega)$ is the difference of susceptibility between the materials a and b; Γ is the ratio of the thickness of material a to the period d.

In the direction Z, the material has a finite size corresponding to N periods. This is taken into account by means of the rectangle function (rect$[(Z-L/2)/L]=1$ for Z between $-L/2$ and $+L/2$ and$=0$ outside). Using the relations (9), (11), and (14), the Hertz vector in far-field is given by

$$\overline{\mathbf{\Pi}}(\mathbf{k},\omega)=\sum_p\overline{\mathbf{\Pi}_p}(\mathbf{k},\omega) \tag{17a}$$

with

$$\begin{aligned}\overline{\mathbf{\Pi}_p}(\mathbf{k},\omega)=\chi_p(\omega)&\int_{-\infty}^{+\infty}dZ\exp[iQ_pZ]\mathrm{rect}\left[\frac{Z-L_0/2}{L_0}\right]\\&\times\left(-\frac{2q}{v\overline{\overline{\varepsilon(\omega)}}}\right)\left(\int_{-\infty}^{+\infty}dX\int_{-\infty}^{+\infty}dY\frac{\partial}{\partial X}[K_0(\alpha_Z\rho)]\right.\\&\times\exp(-i\alpha_{X,p}X)\exp(-i\alpha_Y Y)\hat{\mathbf{X}}\\&+\int_{-\infty}^{+\infty}dX\int_{-\infty}^{+\infty}dY\frac{\partial}{\partial Y}[K_0(\alpha_Z\rho)]\\&\times\exp(-i\alpha_{X,p}X)\exp(-i\alpha_Y Y)\hat{\mathbf{Y}}\\&+\int_{-\infty}^{+\infty}dX\int_{-\infty}^{+\infty}dY\left(\frac{i\alpha_Z^2 v}{\omega}\right)K_0(\alpha_Z\rho)\\&\left.\times\exp(-i\alpha_{X,p}X)\exp(-i\alpha_Y Y)\hat{\mathbf{Z}}\right),\end{aligned} \tag{17b}$$

where use is made of the relation

$$K_1(\zeta)=-\frac{\partial K_0(\zeta)}{\partial\zeta}.$$

In Eq. (17),

$$\begin{aligned}Q_p&=\frac{\omega}{v}-k\sqrt{\overline{\varepsilon(\omega)}}\cos\theta+pg_Z,\\ \alpha_{X,p}&=k\sin\theta\cos\varphi+pg_X,\\ \alpha_Y&=k\sin\theta\sin\varphi,\\ \alpha_Z&=\Lambda,\\ d_0&=d/\sin\alpha,\\ L_0&=Nd_0.\end{aligned} \tag{18}$$

After integration (cf. Appendix C), Eq. (17) becomes

$$\overline{\mathbf{\Pi}_p}(\mathbf{k},\omega)=\chi_p(\omega)\frac{-2iq}{c\beta\overline{\varepsilon(\omega)}}\frac{L_0}{2}\exp\left[iQ_p\frac{L_0}{2}\right]\mathrm{sinc}\left[Q_p\frac{L_0}{2}\right]\times\frac{2\pi}{(\alpha_{X,p})^2+(\alpha_Y)^2+(\alpha_Z)^2}\left\{\alpha_{X,p}\hat{\mathbf{X}}+\alpha_Y\overline{\mathbf{Y}}+\frac{\alpha_Z^2 v}{\omega}\hat{\mathbf{Z}}\right\},\tag{19}$$

where $\mathrm{sinc}\,x=\sin x/x$.

From Eq. (10), the radiated energy is

$$\frac{d^2I}{d\omega\,d\Omega}=\frac{c}{(2\pi)^2}k^4\left|\sum_p\sum_n\{\overline{\mathbf{\Pi}_p^*}(\mathbf{k},\omega)\cdot\overline{\mathbf{\Pi}_n}(\mathbf{k},\omega)-[\overline{\mathbf{\Pi}_p^*}(\mathbf{k},\omega)\cdot\hat{\mathbf{r}}][\overline{\mathbf{\Pi}_n}(\mathbf{k},\omega)\cdot\hat{\mathbf{r}}]\}\right|.\tag{20}$$

Generally, L_0 is sufficiently large so that no overlap exists between terms of different order. Then, by substituting $\mathbf{\Pi}_p(\mathbf{k},\omega)$ from Eq. (19) in Eq. (20), the expression of the energy for a given order p and for both normal and oblique incidences is

$$\begin{aligned}\left(\frac{d^2I}{d\omega\,d\Omega}\right)_p=&\frac{k^4}{c}\frac{q^2}{\beta^2|\overline{\varepsilon(\omega)}|^2}|\chi_p(\omega)|^2L_0^2\left|\mathrm{sinc}\left[Q_p\frac{L_0}{2}\right]\right|^2\\&\times\exp[-L_0\,\mathrm{Im}(Q_p)]\\&\times\left|\frac{1}{(\alpha_{X,p})^2+(\alpha_Y)^2+(\alpha_Z)^2}\right|^2\Big[(\alpha_{X,p})^2\\&\times(1-\sin^2\theta\cos^2\varphi)+(\alpha_Y)^2(1-\sin^2\theta\sin^2\varphi)\\&+\left(\frac{|\alpha_Z^2|v}{\omega}\right)^2\sin^2\theta-2\alpha_{X,p}\alpha_Y\sin^2\theta\sin\varphi\cos\varphi\\&-2\alpha_{X,p}\left(\frac{\mathrm{Re}[\alpha_Z^2]v}{\omega}\right)\cos\theta\sin\theta\cos\varphi\\&-2\alpha_Y\left(\frac{\mathrm{Re}[\alpha_Z^2]v}{\omega}\right)\cos\theta\sin\theta\sin\varphi\Big].\end{aligned}\tag{21}$$

In the limit case where $\overline{\varepsilon(\omega)}$ tends towards unity, Eq. (21) is written as follows:

$$\left(\frac{d^2I}{d\omega\,d\Omega}\right)_p=\frac{q^2}{c}k^2|\chi_p(\omega)|^2L_0^2\left|\mathrm{sinc}\left[Q_p\frac{L_0}{2}\right]\right|^2|F(\theta,\varphi,\omega)|\tag{22}$$

with

$$F(\theta,\varphi,\omega)=\frac{1}{\Delta(\theta,\varphi,\omega)^2}\left[\Delta(\theta,\varphi,\omega)-\left(\frac{\beta}{\gamma}\right)^2-\frac{[\Delta(\theta,\varphi,\omega)+\Sigma(\theta,\omega)]^2}{4\beta^2}\right],\tag{23a}$$

$$\Delta(\theta,\varphi,\omega)=\beta^2\left[\left(\sin\theta+\frac{pg_X}{k}\right)^2-2\sin\theta\frac{pg_X}{k}(1-\cos\varphi)\right],\tag{23b}$$

$$\Sigma(\theta,\omega)=\beta^2\left[\sin^2\theta-\left(\frac{pg_X}{k}\right)^2\right]+\frac{2\beta\cos\theta-1}{\gamma^2}.\tag{23c}$$

III. NORMAL AND OBLIQUE INCIDENCES

A. Normal incidence

For normal incidence,

$$\alpha=\frac{\pi}{2},\quad d_0=d,\quad g_X=0,\quad g_Z=\frac{2\pi}{d},\qquad \alpha_{X,p}=k\sin\theta\cos\varphi.\tag{24}$$

By introducing in Eq. (21) the normal incidence conditions given by Eq. (24) and establishing that $\overline{\varepsilon(\omega)}$ tends towards unity, the intensity reads

$$\frac{d^2I}{d\omega\,d\Omega}=\frac{q^2}{c}k^2|\chi_p(\omega)|^2L^2\left|\mathrm{sinc}\left[Q_p\frac{L}{2}\right]\right|^2|G[\theta,\beta]|^2\tag{25}$$

with

$$G[\theta,\beta]=\frac{\sin\theta(1-\beta\cos\theta-\beta^2)}{1-\beta^2\cos^2\theta}.\tag{26}$$

Equations (25) and (26) are easily identified with the expressions generally used to describe the resonant transition radiation (RTR) emitted by a periodic system [14,16]. From the general expression (21), Cherenkov intensity can also be deduced by setting $p=0$.

It is known that the RTR of wavelength λ/p is emitted in a cone of opening angle denoted 2θ here, centered on the electron trajectory. The resonance condition is obtained when λ/p and 2θ have values such as the ''sinc'' function is maximum, that is, $Q_p=0$. From Eq. (18), we obtain the resonance condition

$$\sqrt{\overline{\varepsilon(\omega)}}\cos\theta_p=\frac{1}{\beta}+p\frac{\lambda}{d}.\tag{27}$$

The angle θ_p is real only for negative values of the integer p. From the variation of $G[\theta,\beta]$ versus β [Eq. (26)] and the condition (27), we have verified that the intensity of the RTR is only significant when the angle between the observation direction and the trajectory of the incident particle is close to $1/\gamma$. Then, for relativistic electrons, the maximum intensity is in the angle of opening $2/\gamma$.

The efficiency of RTR as a radiation source can be deduced from the spatially integrated energy

$$\frac{dI}{d\omega}=\frac{q^2}{c}k^2|\chi_p(\omega)|^2L^2\int_0^{2\pi}d\varphi\int_0^{\pi}\left|\mathrm{sinc}\left[Q_p\frac{L}{2}\right]\right|^2\times|G[\theta,\beta]|^2\sin\theta\,d\theta.\tag{28}$$

The variation of $G[\theta,\beta]$ is slow within the angular width of the function $|\mathrm{sinc}[Q_p(\theta)L/2]|^2$. This behavior is verified all the better that the number of periods N is large. In this case, it is usual to perform the following substitution:

$$\left|\mathrm{sinc}\left[Q_p\frac{L}{2}\right]\right|^2 \rightarrow \frac{2}{L}\pi\delta[Q_p]. \tag{29}$$

Then the integration over θ becomes simple and

$$\frac{dI}{d\omega} \approx \frac{(2\pi)^2 q^2}{c} k|\chi_p(\omega)|^2 L|G[\theta_p]|^2, \tag{30}$$

where θ_p satisfies the resonance condition (27). Equation (29) is generally a convenient approximation. However, let us underline that the value of N is bounded (less than 10^2) and the introduction of the Dirac function is an approximation. Morever, the dielectric constant has been assumed equal to unity. Indeed, in the xuv domain, the dielectric constant is a complex parameter whose imaginary part accounts for the absorption of the radiation by the matter.

B. Oblique incidence

In the general case of oblique incidence, we are able to find another configuration for which an enhanced radiation emission occurs. To do so, we search the conditions for which the intensity becomes maximum. As for the RTR, the ''sinc'' term peaks if $Q_p=0$, i.e., if the resonance condition

$$\sqrt{\overline{\varepsilon(\omega)}}\cos\theta_p = \frac{1}{\beta} + p\frac{\lambda}{d_0} \tag{31}$$

is satisfied. This condition is analogous to Eq. (27) with d_0 instead of d.

1. Limit case: $\overline{\varepsilon(\omega)} \rightarrow 1$

In the limit case where $\overline{\varepsilon(\omega)}$ tends toward unity, it is easy to obtain from Eqs. (22) and (23) the condition leading to a maximum intensity. The derivative of F given by Eq. (23a) is

$$dF = -\frac{d\Delta}{\Delta^2} + 2\left(\frac{\beta}{\gamma}\right)^2\frac{d\Delta}{\Delta^3} + \left[\frac{\Sigma d\Delta - \Delta d\Sigma}{\Delta^2}\right]\left[\frac{1}{2\beta^2}\left(\frac{\Sigma}{\Delta}+1\right)\right]. \tag{32}$$

A sufficient condition for $dF=0$ is

$$\Delta(\theta,\omega) = -\Sigma(\theta,\omega) = 2\left(\frac{\beta}{\gamma}\right)^2. \tag{33}$$

With this condition, the radiated energy reaches a maximum given by

$$\frac{d^2I}{d\omega\, d\Omega} = \frac{q^2}{c}k^2|\chi_p(\omega)|^2 L_0^2\left|\mathrm{sinc}\left[Q_p\frac{L_0}{2}\right]\right|^2\left(\frac{\gamma}{2\beta}\right)^2. \tag{34}$$

Then, in the oblique incidence case, a maximum in the radiated intensity is expected if the conditions (31) and (33) are simultaneously satisfied. By associating to the glancing angle denoted α_p the Bragg wavelength λ_p defined by the Bragg relation

$$2d\sin\alpha_p = |p|\lambda_p, \tag{35}$$

the quantities pg_X/k and pg_Z/k are, respectively, equal to $\lambda/\lambda_p \sin 2\alpha_p$ and $\lambda/\lambda_p 2\sin^2\alpha_p$. Then the wavelength $\lambda_{\max}$ for which the intensity is maximum is given by

$$\lambda_{\max} = \lambda_p\frac{\beta}{2}\left[1+\left(1+\frac{2}{\beta^2\gamma^2\sin^2\theta_{0,p}}\right)^{1/2}\right]. \tag{36}$$

The angles $\theta_{\max}$ corresponding to this maximum are given by

$$\cos\theta_{\max} = \frac{1}{\beta} - \beta\sin^2\alpha_p\left[1+\left(1+\frac{2}{\beta^2\gamma^2\sin^2\alpha_p}\right)^{1/2}\right]. \tag{37}$$

By combining Eqs. (23b) and (33), the azimuthal angles $\varphi_{\max}$ which maximize the intensity can be determined. Both conditions are verified for two opposite values $\pm|\varphi_{\max}|$. Then two directions are expected for maxima of emission; these direction are located symmetrically on each side of the plane of incidence.

In the relativistic case ($\beta\approx 1, \gamma \gg 1$), the conditions (36) and (37) show that enhanced emission occurs in the neighborhood of the Bragg conditions. Indeed

$$\lambda_{\max} \approx \lambda_p\left[1+\frac{1}{2\gamma^2\sin^2\alpha_p}\right], \tag{38}$$

$$\theta_{\max} \approx 2\alpha_p - \frac{1}{\gamma^2\sin 2\alpha_p}. \tag{39}$$

In this case, the energy $dI/d\omega$ is determined by integrating spatially Eq. (22).

This set of formulas displays the advantage of showing simply the general characteristics of the emitted radiation in this geometry.

2. General case

In this case, the radiated energy must be determined by means of Eq. (21). No simple analytical formula can be obtained and numerical treatment must be used. Results of a calculation made for a typical radiator with the true dielectric constant are presented in the next section. From this, we show that the spatial distribution of the radiated intensity is more spread in the direction defined by the angle φ than it is in the limit case $\overline{\varepsilon}\rightarrow 1$. Moreover, at low incident electron energies, the radiated intensity is approximately the same as in the limit case but the variation of the intensity with the electron energy is different. It does not increase with γ as expected from the formula (34), which is no longer valid, and a saturation effect occurs for $\overline{\varepsilon(\omega)} \neq 1$. This saturation starts when the condition $1/(\gamma\beta)^2 \ll 4\pi\overline{\chi}$ is satisfied. Then the parameter Λ, as given by Eq. (12), is practically independent of γ; it tends to the constant value $k\sqrt{4\pi\overline{\chi}}$, so that the electric field radiated by the electron [cf. Eq. (11)] becomes independent of γ, thus of the electron energy.

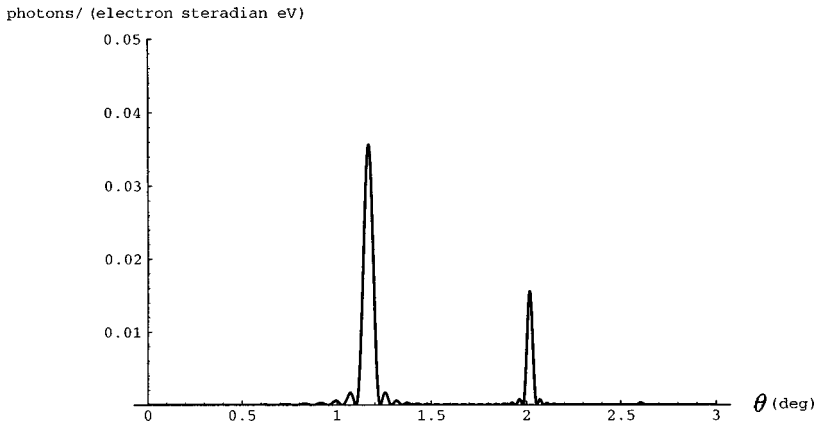

FIG. 2. Angular distribution of the RTR vs the angle θ. The electron energy is 25 MeV. The energy of the photons is 1 keV. The target consists in a periodic arrangement of 1-μm-thick 18 Be foils separated by 2 μm of vacuum.

IV. NUMERICAL APPLICATIONS AND COMPARISON BETWEEN THE VARIOUS RADIATION SOURCES

Numerical applications are made for a radiation of 1 keV($\lambda = 1.24$ nm). In all the cases, we calculate the number of photons radiated per electron, per steradian, in a unit photon energy interval centered about 1 keV.

A. Resonant transition radiation (RTR)

Electrons of 25 MeV ($\gamma = 49$) traveling through a periodic arrangment of 1-μm-thick 18 Be foils separated by 2 μm of vacuum have been previously considered [34]. From Eq. (21), we have calculated the angular distribution of the RTR versus the angle θ for such an arrangement. The result is presented in Fig. 2. The emission occurs in cones centered along the trajectory of the electron with opening angles close to $(2\times1.2)°$ for the first order ($p=1$) and to $(2\times2)°$ for the second order ($p=2$). The third order cancels because the ratio Γ of the foil thickness (1 μm) to the period of the stack (3 μm) is equal to $\frac{1}{3}$ [cf. the expression of χ_p from Eq. (16)]. The number of photons radiated per electron, per eV, per steradian is about 4×10^{-2} while the value calculated from Eq. (1) of Ref. [34] is $\approx 5.6\times10^{-2}$. For this case, the difference between the two values is of the order of magnitude of the imprecision on the optical constants, which can be estimated to be about 20%. Let us underline that our formulation is general while the model of Ref. [34] is valuable only in the x-ray range and for small emission angles.

B. Bragg resonant transition radiation (Bragg RTR) from multilayer systems

Calculation is performed for an existing multilayer structure composed of 35 molybdenum/carbon bilayers [35]. The thicknesses of the Mo and C layers are 1.13 and 2.27 nm, respectively. The stack is deposited onto a 300-nm-thick silicon carbide film. Such thin substrate made up of low-Z elements enables us to reduce the bremsstrahlung emission. At the wavelength of 1.24 nm, the Bragg angle is 10.5° for the order $|p|=1$. We consider a relativistic electron with an energy equal to 25 MeV, impinging the multilayer structure at the Bragg angle. The angular distribution of the radiation versus the angles θ and φ is shown in a 3D plot, Fig. 3(a) for $\varepsilon(\omega)=1$ and Fig. 3(b) for the true value of $\varepsilon(\omega)$, respectively. As expected, the radiation is divided into two peaks corresponding to the two values of $\varphi_{\max}$, separated by a central dip.

In Fig. 4 the peak intensity and the spatially integrated intensity versus the electron energy are plotted simultaneously for $\varepsilon(\omega)=1$ and for the true value of $\varepsilon(\omega)$. As already discussed, saturation appears from 20 MeV for the true value of $\varepsilon(\omega)$. At the peak intensity, the number of photons radiated at 25 MeV is 4×10^{-6} per electron per steradian per eV.

C. Synchrotron radiation

A general expression for the instantaneous power radiated by an electron of energy E at a trajectory point of radius ρ, into all angles, per unit frequency interval centered about the frequency ω, has been derived by Schwinger [38]. In terms of the photon energy $\hbar\omega$ rather than the angular frequency, this expression reduces to

$$P(\hbar\omega,t)=\frac{3^{1/2}}{h}\frac{e^2}{\rho}\left(\frac{E}{m_0c^2}\right)\times\left(\frac{\hbar\omega_c}{\hbar\omega}\right)^2 G\left(\frac{\hbar\omega}{\hbar\omega_c}\right) \quad \text{in C.G.S. units,} \tag{40}$$

where $\hbar\omega_c$ is the so-called critical energy and is defined by the relation

$$\hbar\omega_c=\frac{3}{4\pi}\frac{\hbar c}{\rho}\left(\frac{E}{m_0c^2}\right)^3$$

and the function $G(y)$ is given by

$$G(y)=y^3\int_y^\infty K_{5/3}(\eta)\,d\eta.$$

The integrand in $G(y)$ involves Bessel functions of imaginary argument.

Let us consider an hypothetic machine having its critical energy equal to 1 keV. This is obtained with electrons of about 766 MeV maximum energy moving with constant speed along a circular orbit of 1 m radius. From Eq. (40), one obtains the number of photons radiated per electron averaged

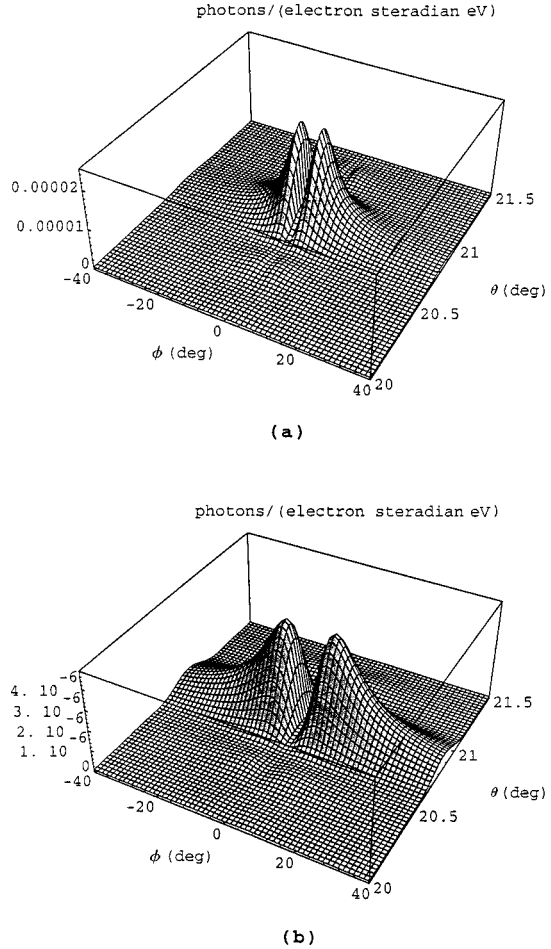

FIG. 3. Angular distribution of the Bragg resonant transition radiation vs the angles θ and φ in a three-dimensional plot. The electron energy is 25 MeV. The energy of the photons is 1 keV. Calculation is performed for a target consisting in a periodic multilayer structure composed of 35 molybdenum/carbon bilayers. The thicknesses of the Mo and C layers are 1.13 and 2.27 nm, respectively. The glancing angle of the incident electron is 10.5°, which is the Bragg angle for photons of energy equal to 1 keV.

on one second and the total energy emitted by the machine is determined by taking into account only the number of electrons present on the orbit at each rotation. Consequently, the number of photons radiated by an electron in a straight moving must be compared with the number of photons radiated by an electron during passing through a point of the orbit; this last is 8×10^{-4} photons per electron per steradian per eV about the critical energy.

V. CONCLUSION

We have shown that resonant transition radiation in normal incidence as well as Bragg RTR from periodic stratified structures can be described by the same theoretical model in the framework of the electromagnetism of continuous media. On the other hand, analogy between Bragg RTR and PXR is evident. Consequently, the use of multilayer stacks as a radiator with a period in the nanometric scale would make possible the extension of the parametric radiation in the xuv domain.

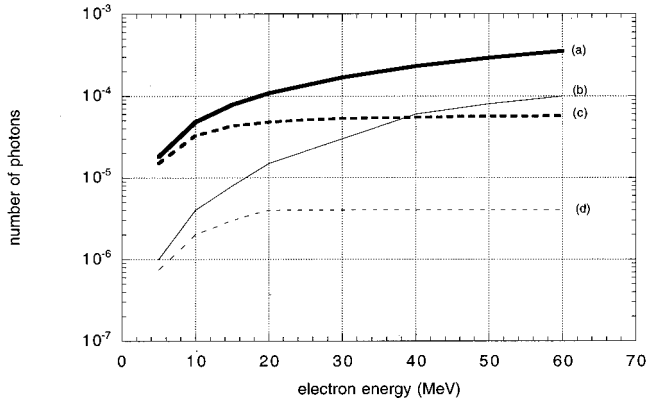

FIG. 4. Number of photons at the peak and spatially integrated number of photons vs the electron energy, for $\overline{\varepsilon(\omega)}=1$ and for the true value of $\overline{\varepsilon(\omega)}$. Curve *a*, spatially integrated number of photons (photons/electron/eV) for $\overline{\varepsilon(\omega)}=1$; curve *b*, number of photons at the peak (photons/electron/steradian/eV) for $\overline{\varepsilon(\omega)}=1$; curve *c*, spatially integrated number of photons (photons/electron/eV) for the true dielectric constant; curve *d*, number of photons at the peak (photons/electron/steradian/eV) for true dielectric constant. The energy of the photons is 1 keV. The target is the same as for Fig. 3.

Performances of various types of sources are difficult to deduce only from the theoretical values calculated in the preceding paragraph. Technical and experimental considerations must be taken into account. Among the technical parameters, average current, temporal, and spatial structures of the incident particle beam are predominant. Thus, in comparison with the synchrotron radiation, insertion devices can increase the intensity by several orders of magnitude. On the other hand, the average current in a storage ring can be two to three orders of magnitude larger than in an electron accelerator. Contrary, the peak current of an electron accelerator is orders of magnitude larger than the current associated to one electron bunch in a storage ring, making the RTR attractive for time-resolved measurements in the x-ray field.

Another important factor is the spectral distribution. In the case of the Bragg RTR, the width of the spectral distribution is narrow, i.e., the radiation is quasimonochromatic, in contrast with the continuous radiation of the synchrotron source. This presents an appreciable advantage in experiments which require a narrow spectral bandwidth.

It must be underlined that the possibility exists to realize multilayer-substrate systems only a few hundred nanometers thick. Such a radiator minimizes the production of bremsstrahlung and the self-absorption and tends to increase the efficiency of the proposed source. Using an electron beam of a few tens of MeV with an average current of 1 mA and a convenient multilayer radiator, a Bragg RTR of 10^{10} photons per second per steradian per unit photon energy interval can be achieved with a spectral broadening of only 10 eV centered about 1 keV. Then Bragg RTR offers the possibility to dispose relatively compact and simple efficient xuv sources for scientific and industrial applications.

APPENDIX A

The electric **E** and magnetic **H** fields are related to the scalar ϕ and vector **A** potentials by

$$\mathbf{E}(\mathbf{r},t)=-\nabla\phi(\mathbf{r},t)-\frac{\partial\mathbf{A}(\mathbf{r},t)}{c\,\partial t}, \tag{A1}$$

$$\mathbf{H}(\mathbf{r},t)=\nabla\times\mathbf{A}(\mathbf{r},t). \tag{A2}$$

From the Maxwell equation

$$\nabla\times\mathbf{H}(\mathbf{r},t)=\frac{\partial\mathbf{D}(\mathbf{r},t)}{c\,\partial t}+\frac{4\pi}{c}\mathbf{J}(\mathbf{r},t), \tag{A3}$$

where $\mathbf{J}$ is the electric current density and $\mathbf{D}$ is the electric displacement vector defined by

$$\mathbf{D}(\mathbf{r},t)=\mathbf{E}(\mathbf{r},t)+4\pi\mathbf{P}(\mathbf{r},t). \tag{A4}$$

One has

$$\nabla\times\mathbf{H}(\mathbf{r},t)=\frac{\partial\mathbf{E}(\mathbf{r},t)}{c\,\partial t}+\frac{4\pi\partial\mathbf{P}(\mathbf{r},t)}{c\,\partial t}+\frac{4\pi}{c}\mathbf{J}(\mathbf{r},t). \tag{A5}$$

If one introduces the electric Hertz vector $\mathbf{\Pi}$ such that

$$\mathbf{A}(\mathbf{r},t)=\frac{\partial\mathbf{\Pi}(\mathbf{r},t)}{c\,\partial t} \tag{A6}$$

and

$$\phi(\mathbf{r},t)=-\nabla\cdot\mathbf{\Pi}(\mathbf{r},t), \tag{A7}$$

then by combining Eqs. (A1), (A2), and Eq. (A5), one finds that the Hertz vector satisfies the following equation:

$$-\nabla^2\frac{\partial\mathbf{\Pi}(\mathbf{r},t)}{c\,\partial t}+\frac{\partial^3\mathbf{\Pi}(\mathbf{r},t)}{c^3\partial t^2}=\frac{4\pi\partial\mathbf{P}(\mathbf{r},t)}{c\,\partial t}+\frac{4\pi}{c}\mathbf{J}(\mathbf{r},t). \tag{A8}$$

Assuming the fields to be harmonics, one obtains

$$\nabla^2\mathbf{\Pi}(\mathbf{r},\omega)+\omega^2\frac{1}{c^2}\mathbf{\Pi}(\mathbf{r},\omega)=-4\pi\mathbf{P}(\mathbf{r},\omega)-i\frac{4\pi}{\omega}\mathbf{J}(\mathbf{r},\omega). \tag{A9}$$

The solution of the above differential equation is obtained by means of the outgoing Green function $G(\mathbf{r},\mathbf{R},\omega)$ of the Helmholtz equation, which verifies

$$\nabla^2G(\mathbf{r},\mathbf{R},\omega)+\omega^2\frac{1}{c^2}G(\mathbf{r},\mathbf{R},\omega)=-4\pi\delta(\mathbf{r}\cdot\mathbf{R}) \tag{A10}$$

by

$$\mathbf{\Pi}(\mathbf{r},\omega)=\int\left[\mathbf{P}(\mathbf{R},\omega)+\frac{i}{\omega}\mathbf{J}(\mathbf{R},\omega)\right]G(\mathbf{r},\mathbf{R},\omega)d^3\mathbf{R}. \tag{A11}$$

It is well known that the Green function $G(\mathbf{r},\mathbf{R},\omega)$ reads

$$G(\mathbf{r},\mathbf{R},\omega)=\frac{\exp\left(i\frac{\omega}{c}|\mathbf{r}-\mathbf{R}|\right)}{|\mathbf{r}-\mathbf{R}|}. \tag{A12}$$

Now we turn to the expression of the magnetic and electric fields in terms of the Hertz vector.

Combining Eq. (A2) and Eq. (A6), it is straightforward to show that in terms of the harmonic field,

$$\mathbf{H}(\mathbf{r},\omega)=-\frac{i\omega}{c}\nabla\times\mathbf{\Pi}(\mathbf{r},\omega). \tag{A13}$$

Combining Eq. (A1), Eq. (A6), and Eq. (A7) yields

$$\mathbf{E}(\mathbf{r},t)=\nabla\nabla\cdot\mathbf{\Pi}(\mathbf{r},t)-\frac{1}{c^2}\frac{\partial^2}{\partial t^2}\mathbf{\Pi}(\mathbf{r},t). \tag{A14}$$

In terms of the harmonic field, one obtains

$$\mathbf{E}(\mathbf{r},\omega)=\nabla\nabla\cdot\mathbf{\Pi}(\mathbf{r},\omega)+\frac{\omega^2}{c^2}\mathbf{\Pi}(\mathbf{r},\omega), \tag{A15}$$

that is,

$$\mathbf{E}(\mathbf{r},\omega)=\nabla\times[\nabla\times\mathbf{\Pi}(\mathbf{r},\omega)]+\nabla^2\mathbf{\Pi}(\mathbf{r},\omega)+\frac{\omega^2}{c^2}\mathbf{\Pi}(\mathbf{r},\omega). \tag{A16}$$

By virtue of Eq. (A9), it comes

$$\mathbf{E}(\mathbf{r},\omega)=\nabla\times[\nabla\times\mathbf{\Pi}(\mathbf{r},\omega)]-4\pi\mathbf{P}(\mathbf{r},\omega)-i\frac{4\pi}{\omega}\mathbf{J}(\mathbf{r},\omega). \tag{A17}$$

At the location of the observator, that is, outside the matter and the electron beam, the electric field is simply given by

$$\mathbf{E}(\mathbf{r},\omega)=\nabla\times[\nabla\times\mathbf{\Pi}(\mathbf{r},\omega)]. \tag{A18}$$

APPENDIX B

The energy detected by a 4π detector (which has a total surface Σ) surrounding the radiator during the experiment is given by

$$I=\frac{c}{4\pi}\int_{-\infty}^{+\infty}dt\int_{\Sigma}\mathbf{dS}\,\mathbf{E}(t)\times\mathbf{H}(t). \tag{B1}$$

Performing a Fourier transform of the electric and magnetic field gives

$$I=\frac{c}{4\pi}\int_{-\infty}^{+\infty}dt\int_{-\infty}^{+\infty}\frac{d\omega}{2\pi}\int_{-\infty}^{+\infty}\frac{d\omega'}{2\pi}\int_{\Sigma}\mathbf{dS}\,\mathbf{E}(\omega)\exp(i\omega t)\times\mathbf{H}(\omega')\exp(i\omega' t). \tag{B2}$$

The integration over time yields

$$I=\frac{c}{4\pi}\int_{-\infty}^{+\infty}\frac{d\omega}{2\pi}\int_{-\infty}^{+\infty}\frac{d\omega'}{2\pi}\int_{\Sigma}2\pi\delta(\omega+\omega')\mathbf{dS}\,\mathbf{E}(\omega)\times\mathbf{H}(\omega'). \tag{B3}$$

The integration over ω' yields

$$I=\frac{c}{2(2\pi)^2}\int_{-\infty}^{+\infty}d\omega\int_{\Sigma}\mathbf{dS}\,\mathbf{E}(\omega)\times\mathbf{H}(-\omega), \tag{B4}$$

that is

$$I=\frac{c}{(2\pi)^2}\int_0^{+\infty}d\omega\int_\Sigma d\mathbf{dS}\,\mathbf{E}(\omega)\times\mathbf{H}^*(\omega). \tag{B5}$$

Consequently, the energy radiated through a elementary surface **dS** per angular frequency interval $d\omega$ is given by

$$\frac{dI}{d\omega}=\frac{c}{(2\pi)^2}|[\mathbf{E}(\omega)\times\mathbf{H}^*(\omega)]\cdot\mathbf{dS}|. \tag{B6}$$

One has

$$\mathbf{E}(\omega)=\boldsymbol{\nabla}\times\boldsymbol{\nabla}\times\boldsymbol{\Pi}(\omega) \tag{B7}$$

and

$$\mathbf{H}(\omega)=-ik\boldsymbol{\nabla}\times\boldsymbol{\Pi}(\omega). \tag{B8}$$

The Hertz vector $\boldsymbol{\Pi}(\omega)$ is expressed by the formula (6) in the main text. In far-field this vector behaves as a plane wave so that one has

$$\boldsymbol{\nabla}\times\boldsymbol{\Pi}(\omega)\approx i\mathbf{k}\times\boldsymbol{\Pi}(\omega). \tag{B9}$$

Consequently,

$$\mathbf{E}(\omega)\times\mathbf{H}^*(\omega)=-\mathbf{k}\times[\mathbf{k}\times\boldsymbol{\Pi}(\omega)]\times-k[\mathbf{k}\times\boldsymbol{\Pi}^*(\omega)]. \tag{B10}$$

Using the identity

$$\mathbf{A}\times(\mathbf{B}\times\mathbf{C})=(\mathbf{A}\cdot\mathbf{C})\mathbf{B}-(\mathbf{A}\cdot\mathbf{B})\mathbf{C} \tag{B11}$$

it follows that

$$\mathbf{E}(\omega)\times\mathbf{B}^*(\omega)=k^4\{[\hat{\mathbf{r}}\cdot\boldsymbol{\Pi}(\omega)][\hat{\mathbf{r}}\cdot\boldsymbol{\Pi}^*(\omega)]-\boldsymbol{\Pi}(\omega)\cdot\boldsymbol{\Pi}^*(\omega)\}\hat{\mathbf{r}}. \tag{B12}$$

Using Eq. (6) yields

$$\frac{dI}{d\omega}=\frac{c}{(2\pi)^2}\frac{k^4}{r^2}|\{[\hat{\mathbf{r}}\cdot\overline{\boldsymbol{\Pi}}(\omega)][\hat{\mathbf{r}}\cdot\overline{\boldsymbol{\Pi}}^*(\omega)]-\overline{\boldsymbol{\Pi}}(\omega)\cdot\overline{\boldsymbol{\Pi}}^*(\omega)\}\hat{\mathbf{r}}\cdot\mathbf{dS}|. \tag{B13}$$

Finally the energy radiated per angular frequency interval $d\omega$ and per steradian $d\Omega$ is given by

$$\frac{d^2I}{d\omega\,d\Omega}=\frac{c}{(2\pi)^2}k^4|\{\overline{\overline{\boldsymbol{\Pi}^*}}(\mathbf{k},\omega)\cdot\overline{\boldsymbol{\Pi}}(\mathbf{k},\omega)-[\overline{\overline{\boldsymbol{\Pi}^*}}(\mathbf{k},\omega)\cdot\hat{\mathbf{r}}]\times[\overline{\boldsymbol{\Pi}}(\mathbf{k},\omega)\cdot\hat{\mathbf{r}}]\}|. \tag{B14}$$

APPENDIX C

The integration over Z is direct and the result is given in terms of the ''$\mathrm{sinc}\,x=\sin x/x$'' function by

$$\frac{L_0}{2}\mathrm{sinc}\left(Q_p\frac{L_0}{2}\right), \tag{C1}$$

where

$$L_0=Nd_0. \tag{C2}$$

The integration over X and Y can be carried out by parts and then the following integrals appear:

$$I_X(\alpha,\eta,b)=\int_{-\infty}^{+\infty}dY\int_{-\infty}^{+\infty}dX\,\frac{\partial}{\partial X}[K_0(b\sqrt{X^2+Y^2})]\times\exp(-i\alpha X)\exp(-i\eta Y), \tag{C3}$$

$$I_Y(\alpha,\eta,b)=\int_{-\infty}^{+\infty}dY\int_{-\infty}^{+\infty}dX\,\frac{\partial}{\partial Y}[K_0(b\sqrt{X^2+Y^2})]\times\exp(-i\alpha X)\exp(-i\eta Y), \tag{C4}$$

and

$$I_Z(\alpha,\eta,b)=\int_{-\infty}^{+\infty}dY\int_{-\infty}^{+\infty}dX\,K_0(b\sqrt{X^2+Y^2})\times\exp(-i\alpha X)\exp(-i\eta Y). \tag{C5}$$

Since the above integral is given by (see below)

$$I_Z(\alpha,\eta,b)=\frac{2\pi}{\alpha^2+\eta^2+b^2}, \tag{C6}$$

it follows that

$$I_X(\alpha,\eta,b)=-i\alpha I_Z(\alpha,\eta,b)=-i\alpha\frac{2\pi}{\alpha^2+\eta^2+b^2}. \tag{C7}$$

and

$$I_Y(\alpha,\eta,b)=-i\eta I_Z(\alpha,\eta,b)=-i\eta\frac{2\pi}{\alpha^2+\eta^2+b^2}. \tag{C8}$$

After introduction of these integrals, Eq. (17) can be rewritten as follows:

$$\overline{\boldsymbol{\Pi}}(\mathbf{k},\omega)=\sum_p\chi_p(\omega)\frac{-2iq}{c\beta\overline{\overline{\varepsilon}}(\omega)}\times\exp\left[iQ_p\frac{L_0}{2}\right]\frac{L_0}{2}\times\mathrm{sinc}\left[Q_p\frac{L_0}{2}\right]\frac{2\pi}{(\alpha_{X,p})^2+(\alpha_Y)^2+(\alpha_Z)^2}\times\left\{\alpha_{X,p}\hat{\mathbf{X}}+\alpha_Y\hat{\mathbf{Y}}+\frac{\alpha_Z^2 v}{\omega}\hat{\mathbf{Z}}\right\}. \tag{C9}$$

Calculation of $I_Z(\alpha,\eta,b)$

$I_Z(\alpha,\eta,b)$ can be rewritten as follows:

$$I_Z(\alpha,\eta,b)=I_Z(t,b)=\int_0^{2\pi}d\phi\int_0^{\infty}K_0(b\rho)\times\exp(-it\rho\cos\phi)\rho\,d\rho \tag{C10}$$

with $t=\sqrt{\alpha^2+\beta^2}$.

Transforming Eq. (C10) leads to

$$I_Z(t,b)=\int_0^\infty K_0(b\rho)\left[\int_0^\pi \exp[v(\rho)\cos\phi]d\phi + \int_0^\pi \exp[-v(\rho)\cos\phi]d\phi\right]\rho\, d\rho, \quad \text{(C11)}$$

where $v(\rho)=-it\rho$.

From Eq. (3.339) of [39], one has

$$I_Z(t,b)=\pi\int_0^\infty K_0(b\rho)\{I_0[v(\rho)]+I_0[-v(\rho)]\}\rho d\rho, \quad \text{(C12)}$$

where I_0 is the Bessel function I of zero order.

Taking into account the relation

$$J_0[iv]=I_0[v], \quad \text{(C13)}$$

where J_0 is the Bessel function J of zero order, and the equation (6.521) of [39], it follows that

$$I_Z(t,b)=\frac{2\pi}{b^2+t^2}=\frac{2\pi}{b^2+\alpha^2+\beta^2}. \quad \text{(C14)}$$

[1] V. L. Ginsburg and I. M. Frank, J. Phys. (Moscow) **IX**, 353 (1945).

[2] M. L. Ter-Mikaelian, *High-Energy Electromagnetic Processes in Condensed Media* (Wiley-Interscience, New York, 1972).

[3] V. L. Ginsburg and V. N. Tsytovitch, *Transition Radiation and Transition Scattering*, Adam Hilger Series on Plasma Physics (Hilger, Bristol, 1990), and references cited therein.

[4] M. L. Cherry, G. Hartmann, D. Müller, and T. A. Prince, Phys. Rev. D **10**, 3594 (1974), and references cited therein.

[5] A. N. Chu, M. A. Piestrup, T. W. Barbee, R. H. Pantell, and F. R. Buskirk, Rev. Sci. Instrum. **51**, 597 (1980).

[6] M. A. Piestrup, D. G. Boyers, C. I. Pincus, J. L. Harris, H. S. Caplan, R. M. Silzer, and D. M. Skopik, Appl. Phys. Lett. **59**, 189 (1991).

[7] M. A. Piestrup, D. G. Boyers, C. I. Pincus, J. L. Harris, X. K. Maruyama, J. C. Bergstrom, H. S. Caplan, R. M. Silzer, and D. M. Skopik, Phys. Rev. A **43**, 3653 (1991).

[8] I. B. Fainberg and N. A. Khizhniak, Zh. Eksp. Teor. Fiz. **32**, 883 (1957) [Sov. Phys. JETP **5**, 720 (1957)].

[9] M. L. Ter-Mikaelyan and A. D. Gazaryan, Zh. Eksp. Teor. Fiz. **39**, 1693 (1961) [Sov. Phys. JETP **12**, 1183 (1961)].

[10] M. A. Piestrup, P. F. Finman, A. N. Chu, T. W. Barbee, R. H. Pantell, G. A. Gearhart, and F. R. Buskirk, IEEE J. Quantum Electron. **QE-19**, 1771 (1983).

[11] M. J. Moran, B. A. Dahling, P. J. Ebert, M. A. Piestrup, B. I. Berman, and J. O. Kephart, Phys. Rev. Lett. **57**, 1223 (1986).

[12] P. Goedtkindt, J.-M. Salomé, X. Artru, P. Dhez, M. Jablonka, N. Maene, F. Poortmans, and L. Warski, Nucl. Instrum. Methods Phys. Res. B **56/57**, 1060 (1991).

[13] H. Backe, S. Gampert, A. Grendel, H.-J. Hartmann, W. Lauth, Ch. Weinheimer, R. Zahn, F. R. Buskirk, H. Euteneuer, K. H. Kaiser, G. Stephan, and Th. Walcher, Z. Phys. A **349**, 87 (1994).

[14] C. T. Law and A. E. Kaplan, Opt. Lett. **12**, 900 (1987).

[15] B. Pardo and J.-M. André, Phys. Rev. A **40**, 1918 (1989).

[16] J.-M. André, R. Barchewitz, C. Bonnelle, and B. Pardo, J. Opt. (Paris) **24**, 31 (1993).

[17] M. S. Dubovikov, Phys. Rev. A **50**, 2068 (1994).

[18] D. Dialetis, Phys. Rev. A **17**, 1113 (1978).

[19] G. Baryshevsky and I. D. Feranchuk, J. Phys. (Paris) **44**, 913 (1983).

[20] I. D. Feranchuk and A. V. Ivashin, J. Phys. (Paris) **46**, 1981 (1985).

[21] Truong Ba Ha and I. Ya Dubovskaya, Phys. Status Solidi B **155**, 685 (1989).

[22] I. Ya. Dubovskaya, S. A. Stepanov, A. Ya Silenko, and A. P. Ulyanenkoff, J. Phys.: Condens. Matter **5**, 7771 (1993).

[23] H. Nitta, Phys. Rev. B **45**, 7621 (1992).

[24] A. Caticha, Phys. Rev. A **40**, 4322 (1989); Phys. Rev. B **45**, 9541 (1992).

[25] Yu. N. Adishchev, S. A. Vorob'ev, B. N. Kalinin, S. Pak, and A. P. Potylitsyn, Zh. Eksp. Teor. Fiz. **90**, 829 (1986) [Sov. Phys. JETP **63**, 484 (1986)].

[26] Yu. N. Adishchev, V. A. Verzilov, A. P. Potylitsyn, S. R. Uglov, and S. A. Vorobyev, Nucl. Instrum. Methods Phys. Res. B **44**, 130 (1989).

[27] R. B. Fiorito, D. W. Rule, X. K. Maruyama, K. L. DiNova, S. J. Evertson, M. J. Osborne, D. Snyder, H. Rietdyk, M. A. Piestrup, and A. H. Ho, Phys. Rev. Lett. **71**, 704 (1993).

[28] S. Asano, I. Endo, M. Harada, S. Ishii, T. Kobayashi, T. Nagata, M. Muto, K. Yoshida, and H. Nitta, Phys. Rev. Lett. **70**, 3247 (1993).

[29] I. Endo, M. Harada, T. Kobayashi, Y. S. Lee, T. Ohgaki, T. Takahashi, M. Muto, K. Yoshida, H. Nitta, A. P. Potylitsin, V. N. Zabaev, and T. Ohba, Phys. Rev. E **51**, 6305 (1995).

[30] J. Freudenberger, V. B. Gavrikov, M. Galemann, H. Genz, L. Groening, V. L. Morokhovskii, V. V. Morokhovskii, U. Nething, A. Richter, J. P. F. Sellschop, and N. F. Shul'ga, Phys. Rev. Lett. **74**, 2487 (1995).

[31] V. V. Morokhovskii, K. H. Schmidt, G. Buschhorn, J. Freudenberger, H. Genz, R. Kotthaus, A. Richter, M. Rzepka, and P. M. Weinmann, Phys. Rev. Lett. **79**, 4389 (1997).

[32] K.-H. Brenzinger, C. Herberg, B. Limburg, H. Backe, S. Dambach, H. Euteneuer, F. Hagenbuck, H. Hartmann, K. Johann, K. H. Kaiser, O. Kettig, G. Knies, G. Kube, W. Lauth, H. Schöpe, and Th. Walcher, Z. Phys. A **358**, 107 (1997).

[33] K.-H. Brenzinger, B. Limburg, H. Backe, S. Dambach, H. Euteneuer, F. Hagenbuck, C. Herberg, K. H. Kaiser, O. Kettig, G. Kube, W. Lauth, H. Schöpe, and Th. Walcher, Phys. Rev. Lett. **79**, 2462 (1997).

[34] P. J. Ebert, M. J. Moran, B. A. Dahling, B. L. Berman, M. A. Piestrup, J. O. Kephart, H. Park, R. K. Klein, and R. H. Pantell, Phys. Rev. Lett. **54**, 893 (1985).

[35] C. Khan Malek, J. Susini, A. Madouri, R. Rivoira, F.-R. Ladan, Y. Lepêtre, and R. Barchewitz, Opt. Eng. (Bellingham) **29**, 597 (1990).

[36] M. Nieto-Vesperinas, *Scattering and Diffraction in Physical*

Optics, Wiley Series in Pure and Applied Optics (Wiley, New York, 1991).

[37] J. D. Jackson, *Classical Electrodynamics*, 2nd ed. (Wiley, New York, 1975), p. 634.

[38] J. Schwinger, Phys. Rev. **75**, 1912 (1949).

[39] I. S. Gradshteyn and I. M. Ryzhik, *Tables of Integrals, Series and Products*, 5th ed., edited by A. Jeffrey (Academic, Boston, 1994).